Validation Methods for Industrial Machine Learning Problems

Trabajo Fin de Grado

Grado en Ingeniería Aeroespacial

Escuela Técnica Superior de Ingeniería
Aeronáutica y del Espacio

Universidad Politécnica de Madrid

Autor: Pablo Yeste Blesa

Tutor académico: Javier de Vicente Buendía

Marzo 2024

Resumen.

Las matrices de transición de estado constituyen una herramienta muy útil para el análisis de movimiento relativo entre vehículos espaciales. El hecho de ser formas lineales y además de soluciones semianalíticas se plasma en las siguientes ventajas:

a. Dan lugar a un coste computacional razonable, sin comprometer en exceso la precisión numérica.

b. Su carácter analítico permite extraer conclusiones interesantes sobre el funcionamiento del sistema.

Los modelos linealizados generalmente permiten obtener mejores resultados mediante una mejor modelización del sistema. En el caso de la dinámica espacial relativa, el análisis y la implementación de perturbaciones son vitales, al ser la parte normalmente despreciada y más difícil de modelar del problema. Uno de los efectos más comúnmente analizados en el caso de órbitas terrestres es el campo gravitatorio no esférico, debido esencialmente a ser el más relevante en magnitud en órbitas bajas. La expansión del potencial gravitatorio en armónicos esféricos permite obtener una aproximación ciertamente precisa del mismo, aunque, en función de cómo se aborde, su manejo analítico puede resultar altamente complejo.

Este trabajo trata de proporcionar una visión general sobre la dinámica relativa linealizada entre vehículos espaciales, analizando modelos progresivamente más complejos y precisos, así como introduciendo teorías de perturbaciones – cuyo uso último es la construcción de modelos para dinámica relativa. El concepto de seguridad orbital también es abordado, debido a su vital importancia en el movimiento relativo en cercanía (p.ej., vuelo en formación, *rendez-vous*...).

Abstract.

State Transition Matrices are a very useful and widely used tool for the analysis of linearised spacecraft relative motion. Their closed-form and linear characters bear two main advantages:

    a. A quite good computational cost is achieved, without compromising accuracy more than desired.

    b. Highly insightful knowledge about the dynamics of the system is obtained.

Linearised models return better outcomes the truer-to-life they are. With this in mind, the analysis and implementation of perturbations play an important role, as it is one of the main ways to achieve high accuracy. Earth's non-spherical gravity field is by far the most usually analysed perturbation in Earth orbits, as it has generally the biggest effect (in value). The way in which this perturbation is approached allows for a better or worse reliability of the results.

This thesis intends to provide an outlook on linearised relative motion, evaluating increasingly more complex motion models, and also analysing perturbation theories, whose ulterior use is relative motion. Orbit safety is also recurrently tackled, due to the vital role it plays in close-proximity relative motion.

Contents

Nomenclature

Acronyms

BF   Body-Fixed frame

CR3BP   Circular Restricted Three Body Problem

CW   Clohessy-Wiltshire

ECEF   Earth-Centered Earth-Fixed frame

ECI   Earth-Centered Inertial frame

GA   Gim-Alfriend

HCW   Hill/Clohessy-Wiltshire

Hi-Fi   High-Fidelity

ICs   Initial Conditions

IP   In-plane

IVP   Initial Value Problem

KOE   Keplerian OEs vector

LEO   Low Earth Orbit

LVLH   Local-Vertical, Local-Horizontal frame

MOD   Mean-of-Date frame

NSG   Non-spherical gravity

ODE   Ordinary Differential Equation

OEs   Orbital Elements

OOP   Out-of-plane

PBF   Pseudo-Body-Fixed frame

RTN   Radial-Transverse-Normal frame

SRP   Solar Radiation Pressure

STM   State Transition Matrix

TOD   True-of-Date frame

YA   Yamanaka-Ankersen

General

μ	Gravitational parameter of a celestial body	$\left[\frac{m^3}{s^2}\right]$
$\underline{a}_i$	Acceleration on body i	$\left[\frac{m}{s^2}\right]$
$\underline{F}_i$	Force on body i	$[N]$
a_e	Equatorial radius of a celestial body	$[m]$
m_i	Mass of body i	$[kg]$

Mathematics

$\Delta\bullet$	Variation or increment of a quantity
$\delta\bullet$	Relative quantity (deputy's minus chief's value)
Λ	Real or complex eigenvalue matrix
$\mathbb{I}$	Identity matrix
$\Phi(t,t_0)$	State Transition Matrix
J	Jordan form
V	Real or complex eigenvector matrix
$\boldsymbol{A}$	System's matrix of a system of ODEs
$\underline{f}$	Dynamics function of a system
$\underline{u}, \underline{y}$	State vector of a system of ODEs

Orbital elements

λ	Mean argument of latitude	$[rad]$
Ω	Right Ascension of Ascending Node	$[rad], [deg]$
ω	Argument of periapsis	$[rad], [deg]$
θ	True anomaly	$[rad], [deg]$
a	Semimajor axis	$[m]$
E	Eccentric anomaly	$[rad]$
e	Eccentricity	$[---]$
F	Eccentric argument of latitude	$[rad]$
i	Inclination	$[rad], [deg]$
M	Mean anomaly	$[rad]$

| u | True argument of latitude | $[rad]$, $[\deg]$ |

Perturbations

$\overline{OE}$	Mean orbital element vector	
$\underline{OE}$	Osculating orbital element vector	
ε	Small parameter	$[---]$
H	Hamiltonian of the system	
K	Modified Hamiltonian of the system	
p_i, P_i	Generalized momentum (original or transformed)	
q_i, Q_i	Generalized coordinate (original or transformed)	
R	Disturbing function	?
S, W	Generating function of the transformation	

Subindices

$\bullet_0$	Variable at $t = t_0$
$\bullet_C$	Variable from the chief spacecraft
$\bullet_D$	Variable from the deputy spacecraft
$|_i$	Expressed in frame i

Useful expressions

$\eta = \sqrt{1 - e^2}$		$[---]$
ϕ, λ	Geodetic latitude and longitude	$[rad]$, $[\deg]$
$\rho = 1 + e\cos\theta$		$[---]$
h	Orbit altitude or orbit momentum	$[m]$ or $\left[\dfrac{m^2}{s}\right]$

List of Figures

List of Tables

Introduction.

Spacecraft relative motion is an essential part of distributed space systems analysis. It focuses on the dynamics of two or more vehicles, whose relative position (and generally attitude) should be controlled or at least monitored. Rendez-vous operations, formation flying and satellite constellations are three examples of relative motion, all of them being present in contemporary and past missions. Its relevance cannot be underestimated, and its complexity leads to the currently non-existent quorum on its modelling. However, it is quite widely accepted that linear models using State Transition Matrices (*i.e.* STMs onwards) provides a comforting balance between accuracy and computational cost. One could think that, given the huge computational resources that most people have access to, computational efficiency should not even be a concern. Be that as it may, satellites on-board computers have limited resources, both computational and energy-related. Any reduction in any activity is greatly welcomed, and that naturally includes the GNC computation. That is the reason why this thesis focuses on the review, analysis and implementation of STM models of relative motion.

A bottom-up approach to this topic is herewith followed, starting from the simplest relative motion model (HCW), building up complexity with elliptic models (YA) and finally reaching state-of-the-art perturbed models. With respect to perturbations, non-spherical gravity arises as the main concern, due to its prevailing effect over the other sources - third bodies and drag among others - for the Earth-centered orbits (excluding very low LEO orbits or very high orbits, like GEO).

Chapter 1 provides a brief description of the roots of this thesis. Relative motion and its main branches are firstly described, to then continue with STMs and its applications.

Chapter ?? starts with the development of the equations of relative motion, eventually reaching Hill equations, which model the linearised equations for circular unperturbed reference orbits. Several approaches to its solution are detailed, performing then a small trade-off analysis between them. Finally, orbit safety is presented, to be then applied to the circular, unperturbed case.

Chapter ?? looks for extending the analysis to elliptic (still unperturbed) reference orbits. The state-of-the-art Yamanaka-Ankersen model is developed and tested against a High-Fidelity propagator. To end this chapter, the safe orbit theory is also extended to this elliptic case, through the usage of an analogue set of relative orbital elements and a slightly different relative reference frame.

Chapter ?? tackles the analysis of propagation theory. A brief analysis of averaging methods is discussed, including Von Zeipel's and Lie series' approach. Afterwards, the spotlight is turned on the non-spherical gravity field modelling. The classical Brouwer's theory is first briefed, to then move on to probably the main topic of the thesis: Kaula's theory, which tries to develop a general approach to the spherical harmonic description of the gravity field.

After this theoretical analysis, **chapter ??** moves back to the relative motion field, considering perturbations in this case. An implementation of Brouwer's theory is drafted through Gim-Alfriend STM, after which a survey of the state of the art of perturbed relative motion is presented. To conclude, perturbed orbit safety is simply sketched out.

The pure content of the thesis is then followed by a set of appendices to provide some background in certain relevant topics, if that is required or desired by the reader.

Appendix A provides a comprehensive review and description of the main orbital element sets.

In a somewhat parallel fashion, **appendix ??** focuses on the reference systems used or mentioned throughout the thesis, as well as the transformations between them and from/to orbital elements.

The variational formulation of the spacecraft equations of motion is introduced in **appendix ??**, providing context for some subjects of perturbation theory.

Appendix ?? is devoted to the software approach and structure of the developed content during the thesis.

Finally, **appendix ??** contains several relevant topics that are not big enough to be included in an individual appendix, and do not fully fit into the existing ones.

The goal of this thesis is then to provide an educated outlook on the linearised formulation of spacecraft relative motion, building up complexity as it unfolds, eventually reaching state-of-the-art models which are actually used in operational missions. Due to the structure of this field, this finds a niche in the manipulation and understanding of perturbations; as a result of which a considerable part of the thesis is devoted to it. The validation and trade-off evaluation of said models is naturally an essential part of this work as well. However, this thesis is not a result-based work: it is rather a knowledge, analysis-based project, which should be kept in mind along its reading.

The Validation Loop

1.1 Introduccion

Spacecraft relative dynamics is a vast, very relevant and ever-increasing branch of celestial mechanics. It tries to analyse, rather than the motion around a central body, that of a secondary body (or set of bodies) around a primary, assuming that neither of them generate a gravitational effect on each other. This discipline hence focuses on analysing how a certain force field – which may include different influences – differentially affects two or more different spacecrafts in a mostly common orbit.

1.2 Train-test split

1.2.1 Preliminaries

In supervised learning applications, the dataset is typically divided into the training, the validation, and the test set. Each set is used for different tasks, namely: training, model validation and hyperparameter tuning. Keeping different sets for each task is fundamental in order to prevent model bias. Typical figures for the train-validation-test split are 60%-20%-20%[1, pp. 20-21].

Training and evaluating the NN on the same dataset would result in the phenomenon called overfitting[1, pp. 19-20], which basically consists of the NN fitting the noise in the training data and thus losing performance on unseen data (inference ability).

With the dataset split into the train, evaluation, and test sets, the standard training and validation loop is as follows: the model is trained to "fit" the data in the training set. After a certain amount of training, its performance is measured on the evaluation set. The test set is used to compare the performance of different hyperparameter configurations. Note that the NN is always evaluated with data not previously "seen" during training, and as such cannot develop any bias for the training set (although bias for the validation or test sets may exist).

In the model validation loop, the first question that should be asked, even before training the model, is whether the dataset split is appropriate for training.

For our case of applicability (MSP18, explicar en otra seccion), we suppose we have a dataset which has been split into a training set

$$\mathcal{S}_{\text{train}} = \{(\mathbf{X^{tr}}, \mathbf{Y^{tr}})_i\}_{i=1}^{N_{training}}$$

and a test set

$$\mathcal{S}_{\text{test}} = \{(\mathbf{X^{te}}, \mathbf{Y^{te}})_i\}_{i=1}^{N_{test}},$$

where $\mathbf{X} = (X_1, X_2, \ldots, X_m)$ is the vector of input variables (also called feature vector), m is the dimensionality of the input parameter space, and $\mathbf{Y} = (Y_1, Y_2, \ldots, Y_q)$ is the vector of output variables, with dimensionality q. Individual variables X_k can be numerical or categorical. For instance, for stress problems such as MSP-S18, we have a combination of numerical (*e.g.* external loads) and categorical (eg discrete geometrical variables such as "Frame" or "Stringer", and purely categorical such as "dp"). Individual variables Y_k describe the prediction and these are typically numerical (for stress problems such as MSP-S18, $q = 6$ and these are so-called reserve factors, quantifying the failure likelihood of different failure modes).

The aim of this section is to propose a set of tests to evaluate to which extent splitting fulfils the necessary conditions for the subsequent surrogate model $\hat{\mathbf{Y}} = \hat{F}(\mathbf{X})$ to be appropriately trained on $\mathcal{S}_{\text{train}}$ and tested on $\mathcal{S}_{\text{test}}$.

1.2.2   The train-test split problem in supervised learning

For evaluation purposes, the idea should be kept in mind that the surrogate model is just a parameterized nonlinear approximator of a function $\mathbf{Y} = F(\mathbf{X})$. Let $\mathcal{D}$ be the dominium of the function F, of which only a fraction is available for training and evaluating purposes, *i.e.* $\mathcal{S}_{train}, \mathcal{S}_{test} \subseteq \mathcal{D}$. Logically, it is desirable that $\mathcal{S}_{train}$ and $\mathcal{S}_{test}$ be statistically as close as posible to $\mathcal{D}$ and to each other in order for the training and validation of the model to be coherent. Nonetheless, the statistical similarity with $\mathcal{D}$ is an off-design problem, meaning once $\mathcal{S}_{train}$ and $\mathcal{S}_{test}$ are set a surrogate model $\hat{F}$ can be developed accordingly to perform well at least over a dominium which is said to be in the interpolating region of $\mathcal{S}_{train}$. The concept of interpolating regime is of great importance for surrogate models and shall be further discussed later. On the other hand, the statistical similarity of $\mathcal{S}_{train}$ and $\mathcal{S}_{test}$ is a design problem, meaning if $\mathcal{S}_{test}$ is not in the interpolating region of $\mathcal{S}_{train}$ then the surrogate model $\hat{F}$'s performance over a dominium in the interpolation region of $\mathcal{S}_{train}$ is not guaranteed. In

other words, no trustworthy evaluation of the model can be carried out. It is this in-design problem of statistical accordance between $\mathcal{S}_{train}$ and $\mathcal{S}_{test}$ the one addressed here.

A proper definition of statistical accordance between two sets in the context of $\mathcal{S}_{train}$ and $\mathcal{S}_{test}$ is therefore needed, which will in the end take us to the concept of interpolation. An evidently conservative condition for assuring statistical equivalence can be expressed by the equation (1.1):

$$P_{training}(\mathbf{x}) = P_{test}(\mathbf{x}) \tag{1.1}$$

where $\mathbf{x} = (x_1, x_2, x_3, ..., x_m)$ is the vector of input variables.

In fact, the condition given by (1.1) indeed assures statistical equivalence between the two sets, nonetheless is impossible to fulfil given that $\mathcal{S}_{train} \cap \mathcal{S}_{test} = \emptyset$ by definition. Instead, we will see that the goodness of the train-test split is closely related to the idea of interpolation. We now of NN that they perform well they work in interpolation regime. There is a subtle nuance here that our knowledge of NNs suggests not only NNs perform well at interpolating, but that they perform well *because* they interpolate, *i.e.* they cannot perform well at non-interpolating tasks, or at least it is not possible to statistically assure their performance. This is a matter of discussion highly debated in the literature (see *e.g.* [2–4]).

Subsequently, we want to be sure that our surrogate model is indeed interpolating when evaluating its performance. This idea of interpolation constitutes a basis for the proposed train-test split validation analysis, *i.e.* the train-test split is sufficiently good whenever $\mathcal{S}_{test}$ falls in the interpolation region of $\mathcal{S}_{train}$.

There are plenty of definitions for the interpolating region of a given dataset. Some authors define it as the smallest hypercube enclosing the data[5] although this might lead to points well faraway from the training set being considered to fall inside the interpolation region. Many authors (see v. gr. [6, 7]) define the interpolation region as the *convex hull* of the training data, *i.e.* :

Definition 1. *[8] Standard interpolation occurs for a sample* $\mathbf{x}$ *whenever this sample belongs to the convex hull of a set of samples* $\mathbf{X} \triangleq \{\mathbf{x}_1, ..., \mathbf{x}_N\}$.

The convex hull can be simply defined as the smallest convex set containing the data[9].

Recently, [8] have pointed out that, due to the so-called curse of dimensionality, extrapolation outside the training convex hull always ends up taking place if the input dimension is sufficiently high. The curse of dimensionality[1, pp. 17-18] can be illustrated by the fact that the unitary n-hypersphere's volume asymptotically diminishes to 0 as n increases. In the end, the effect is that, as

the number of dimensions increase, more data is needed in order for the model to work in interpolating regime, as shows :

Theorem 1.2.1. *[10] Given a d-dimensional dataset* $\mathbf{X} \triangleq \mathbf{x}_1, ..., \mathbf{x}_N$ *with i.i.d. samples uniformly drawn from a hyperball, the probability that a new sample* $\mathbf{x}$ *is in interpolation regime (recall 1) has the following asymptotic behavior:*

$$\lim_{d \to \infty} p(\mathbf{x} \in Hull(\mathbf{X})) = \begin{cases} 1 & \iff N > d^{-1}2^{\frac{d}{2}} \\ 0 & \iff N < d^{-1}2^{\frac{d}{2}} \end{cases} \tag{1.2}$$

Studies from [8] seemed to contradict previous knowledge on the importance of interpolation in NNs performance.

The main answer arosen to the argument of [8] is that interpolation does not occur in the ambient space, but in a latent, low-dimensional space of the input data[11]. This leads to a new definition of interpolation alternative to 1.

What's more, the authors in [11] not only show that interpolation indeed occurs (at least in a latent representation of the ambient space), but that more important conditions to the model's performance are that unseen and training data follows the same cumulative distribution (or the same tail distribution when the former cannot be fulfiled) and that the average distance between training points is similar to the average distance between training and testing points.

1.2.3   Proposed validation loop for the train-test

A validation loop for the train-test split is given in the form of a flux diagram whose nodes are different tests aimed at checking statistical properties which characterize the split as has been discussed in the previous section. The diagram derives the results of the tests to apropriate recommendations given to the data engineer. Before showing the complete loop, it is convenient to state the nomenclature conventions used in the diagram for the sake of clarity:

Definition 2. *Let* $\mathbf{X}$ *represent some dataset, which has been split in* $\mathbf{X}^{TRAIN}$ *and* $\mathbf{X}^{TEST}$. $\mathbf{X}$ *is said to be order 1 [O(1)] well-split if and only if* $\mathbf{X}^{TEST} \subseteq Hull[\mathbf{X}^{TRAIN}]$.

Where we denote the convex hull of $\mathbf{X}^{TRAIN}$ by $Hull[\mathbf{X}^{TRAIN}]$.

Definition 3. *Let* $\mathbf{X}$ *represent the dataset defined in* 2. $\mathbf{X}$ *is said to be order 2 well-split if and only if*

1.3 Las movidas de Rodrigo

Orbit propagation is a very wide and varied field. It comprises many different approaches and methods to obtain more or less accurate results, with a higher or lower computational cost. Some examples are the numerical integration of the equations of motion in cartesian coordinates, the numerical integration of the variational equations (*i.e.* equations of motion expressed in OEs) and the development of closed-form solutions by simplifying the problem. Within this last group, State Transition Matrices arise.

The State Transition Matrix is a linearization procedure of a nonlinear dynamical system. It is used to approximate the dynamics of said system over short periods of time, allowing for a lower computational cost while maintaining an acceptable accuracy. This concept is not restricted to orbital mechanics, although it is one of the main fields in which it is used [12].

This section intends to provide some background in (a) its mathematical formulation and (b) its applications in orbit theory.

1.3.1 Concept: System dynamics.

Consider the uncontrolled, nonlinear dynamic system that is characterized through the state vector $\underline{y} = [y_1, y_2, \ldots, y_n]$. The Initial Value Problem (IVP) for this system may be expressed as:

$$[P] \equiv \begin{cases} \text{Eq.} & \dfrac{d\underline{y}}{dt} = \boldsymbol{F}(\underline{y}, t) \\ \text{ICs.} & \underline{y}(t_0) = \underline{y}_0 \end{cases} \tag{1.3}$$

where $\boldsymbol{F}(\underline{y}, t)$ represents the nonlinear dynamics of the system. This problem is unsolvable in general, mainly due to its nonlinearity. In the context of orbit propagation, the state vector $\underline{y}$ might be the position and velocity (be it relative or absolute) of the celestial body, and the dynamics function $\boldsymbol{F}$ contains the considered force model. In order to arrive at a closed-form, solvable problem, it is assumed that the solution $\underline{y}(t)$ can be expressed as:

$$\underline{y}(t) = \Phi(t, t_0)\underline{y}(t_0) \tag{1.4}$$

where $\Phi(t, t_0)$ is the State Transition Matrix (STM) of the system. This matrix allows the state vector at a certain epoch t to be calculated as the product of the matrix times the initial condition. This expression is obviously very favorable, but the question now is how does one compute it. Its actual definition can be easily derived from (1.4) as:

$$\Phi(t, t_0) \equiv \frac{\partial \underline{y}}{\partial \underline{y}_0} \tag{1.5}$$

Yet again, how to compute it is not clear at all. There are three main options, depending on the situation:

A. If the nonlinear solution as a function of the initial condition is known, then the expression (1.5) is directly applied. This is an uncommon case, although simplified examples exist in the orbit propagation field. For example, the Keplerian motion equations expressed in Keplerian orbital elements (OEs) can be solved this way, due to the trivial remaining equations. Another example is the Clohessy-Wiltshire solution, from which the STM can be directly obtained. This process is detailed later on in section **??**.

B. The nonlinear solution is unknown in the original state space, but can be calculated in a different space through a transformation. Mathematically, this can be written as:

$$\Phi_y(t, t_0) = \frac{\partial \underline{y}}{\partial \underline{y}_0} = \frac{\partial \underline{y}}{\partial \underline{u}} \frac{\partial \underline{u}}{\partial \underline{u}_0} \frac{\partial \underline{u}_0}{\partial \underline{y}_0} \equiv W(t) \Phi_u(t, t_0) \left(W(t_0) \right)^{-1} \tag{1.6}$$

where $W(t)$ is the transformation matrix, where it is assumed that the transformation $\underline{y} = h(\underline{u})$ is known. An example of this kind of approach is the transformation of the Cartesian equations of motion into the Keplerian OEs, whose solution is known, as mentioned in A.. This is a very commonly used method in relative orbit propagation, as in [13, 14].

C. If none of the above can be performed, then the STM can be integrated itself, to be then used to calculate the state vector. This starts by differentiating (1.3) with respect to the initial condition $\underline{y}_0$, leading to:

- $\dfrac{\partial}{\partial \underline{y}(t_0)} \dfrac{d\underline{y}(t)}{dt} = \dfrac{d}{dt} \dfrac{\partial \underline{y}(t)}{\partial \underline{y}(t_0)} = \dfrac{d}{dt} \boldsymbol{\Phi}(t, t_0)$

- $\dfrac{\partial \boldsymbol{F}(t, \underline{y})}{\partial \underline{y}(t_0)} = \dfrac{\partial \boldsymbol{F}(t, \underline{y})}{\partial \underline{y}(t)} \dfrac{\partial \underline{y}}{\partial \underline{y}(t_0)} = \boldsymbol{A}\boldsymbol{\Phi}(t, t_0)$

$$\Rightarrow [P] \equiv \begin{cases} \text{Eq.} & \dfrac{d}{dt}\Phi(t,t_0) = \boldsymbol{A}\Phi(t,t_0) \\ \text{IC} & \Phi(t_0,t_0) = \mathbb{I}_{nxn} \end{cases} \tag{1.7}$$

This last method is a bit unrewarding, as it forces one to integrate an IVP. However, the problem in terms of $\Phi(t,t_0)$ (eq. (1.7)) might be simpler or more efficient than the original (eq. (1.3)), although it is rare. An example of this approach is shown later in section **??**.

1.3.2 Applications of STMs in celestial mechanics.

State Transition Matrices can be useful in a wide range of spacecraft dynamics applications. Some of the most important are [15]:

A. Precise Orbit Determination.

Precise Orbit Determination (POD) is a method through which the orbit of a flying spacecraft can be determined with a high accuracy [16]. This estimation is performed using general orbit determination algorithms, such as Kalman filtering or a batch least squares. It requires both high-precision geodetic receivers and high-precision dynamics models, where STMs comes to play. POD usually requires all typically important perturbations, such as non-spherical gravity, drag, tidal forces ...

B. Guidance, Navigation and Control (GNC).

GNC deals with the design the systems to control the spacecraft. It involves the determination of the desired trajectory (guidance), the instantaneous determination of the spacecraft's position (navigation) and the manipulation of the controllers to execute guidance commands (control). STMs become very useful specially in situations in which the linearization error is small, such as in rendez-vous, station-keeping or formation flying operations. They prove to be useful in all three branches:

- Guidance: STMs are a lightweight yet precise tool to generate reference trajectories.

- Navigation: Signal filtering makes extensive use of STMs for the propagation of the estimated state. This is certainly one of the most relevant applications.

- Control: Algorithms like robust online optimal control involve state propagation, using the STM.

C. Orbit design.

Alternatively, rather than propagating already defined orbits, it may be useful to solve the inverse problem: that is, find the orbit that satisfies a set of conditions (*e.g.* optimality). This is specially relevant for the Circular Restricted Three Body Problem (CR3BP), or its particular case of Halo orbits

(periodic 3D orbit near one of the Lagrange libration points). STMs are quite useful to determine an initial solution for said Halo orbits, and can also be used to evaluate the effect of a deviation in initial conditions or other parameters.

Some degree of uncertainty will always be assumed in the estimation of a spacecraft's position and velocity. This matter becomes really important in the context of collision avoidance, where ideally, said uncertainty would be exactly calculated. However, these values are usually not something inherently worrying. What is worrying indeed is that this uncertainty may propagate in a divergent fashion, leading to unbounded trajectories with its inherent collision risk.

Here is where the covariance matrix comes to light. Conceptually, it can be seen as an entity which indicates how certain are each of the components of the state vector. That is represented by their variances and covariances. Mathematically, it is defined as:

$$P(t) = E\left[\left(\hat{\underline{x}} - \underline{x}\right)\left(\hat{\underline{x}} - \underline{x}\right)^T\right]$$

If one knew the covariance at a certain epoch t_j, it is possible to map it to a different epoch t_k (latter or earlier) through the STM, that is:

$$P(t_k) = E\left[\left(\hat{\underline{x_k}} - \underline{x_k}\right)\left(\hat{\underline{x_k}} - \underline{x_k}\right)^T\right] = E\left[\Phi(t_k, t_j)\left(\hat{\underline{x_j}} - \underline{x_j}\right)\left(\hat{\underline{x_j}} - \underline{x_j}\right)^T \Phi^T(t_k, t_j)\right]$$

$$\Rightarrow P(t_k) = \Phi(t_k, t_j)P(t_j)\Phi^T(t_k, t_j)$$

Now, once the mathematical formalism has been stated, it is time to apply it to the situation at hand. Spacecraft state uncertainty has essentially two sources: estimation error (associated to navigation) and execution error (associated to control/manoeuvres).

In a fairly relaxed approach (*i.e.* assuming the state variables be decoupled), the covariance matrix associated to the estimation error has the following shape:

$$P_{est} = \begin{bmatrix} \delta x^2 & 0 & 0 & 0 & 0 & 0 \\ 0 & \delta y^2 & 0 & 0 & 0 & 0 \\ 0 & 0 & \delta z^2 & 0 & 0 & 0 \\ 0 & 0 & 0 & \delta v_x^2 & 0 & 0 \\ 0 & 0 & 0 & 0 & \delta v_y^2 & 0 \\ 0 & 0 & 0 & 0 & 0 & \delta v_z^2 \end{bmatrix} \tag{1.8}$$

where $\delta\psi$ indicates the standard deviation of the variable ψ. An useful way to visualize the covariance is the probability ellipsoid, defined by:

$$\begin{bmatrix} \tilde{x} & \tilde{y} & \tilde{z} \end{bmatrix} P_{xyz}^{-1} \begin{bmatrix} \tilde{x} \\ \tilde{y} \\ \tilde{z} \end{bmatrix} = l^2$$

where $\tilde{x}, \tilde{y}, \tilde{z}$ are the coordinates of a point of the ellipsoid (referred to its center), P_{xyz} is the partition of the covariance matrix related to the position and l is the sigma coefficient. That is, for $l = 2$, the equation represents the ellipsoid in which the spacecraft will be found with a 2σ probability. An example of the evolution of this ellipsoid can be seen for a small radial hop in figure 1.1.
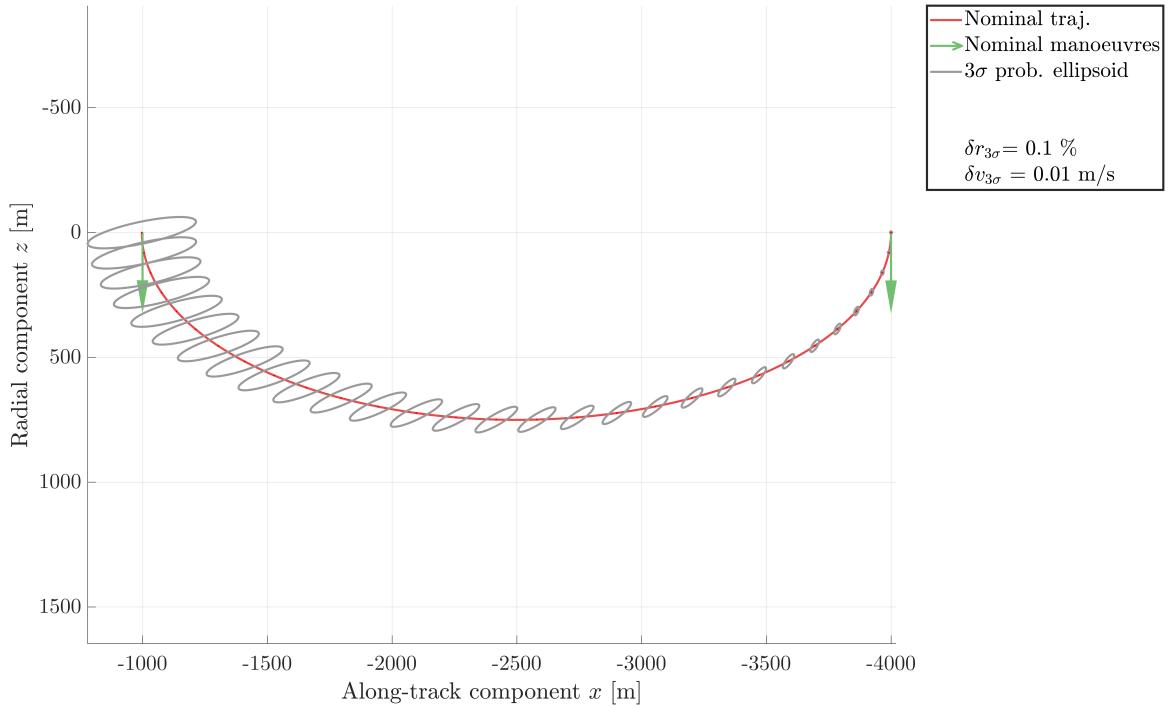

Figure 1.1: Covariance ellipsoid evolution along a radial hop.

Most of these concepts lie out of the thesis' scope. However, it is important to know that the STMs developed or quoted throughout this thesis can be used in many different fields of celestial mechanics.

Conclusions and research outlook.

The increasingly higher relevance of relative motion is beyond question. Satellite constellations, rendezvous operations and formation flying missions are becoming an everyday occurrence, and their growing success rates are no coincidence. Incrementally better models (*i.e.* truer-to-life, accounting for more effects) have an essential role in this.

In order to gain a comprehensible insight on this topic, this thesis has followed the same bottom-up structure, starting from the very simple Hill/Clohessy-Wiltshire equations up to the modelling of perturbations. The use of linear, closed-form models (through STMs) is an advantageous approach: firstly, computational cost drops, but even more importantly, deeper knowledge about the dynamics of the system is achieved. This allows for, among other things, the design of relative orbits with certain characteristics (*e.g.* safe orbits).

Any state-of-the-art model requires an analysis of the relevant perturbations to be carried out. For the case of Earth artificial satellites, this usually leaves the non-spherical gravity as the most important of them. Kaula's theory allows for the analysis of the effect of any spherical harmonic, which naturally leads for better accuracy models. Although it features certain singular cases (resonances and circular or equatorial orbits), these can be solved. Many applications can be branched from this theory, such as mean-to-osculating transformations, linearized relative motion models, resonance analysis . . .

In conclusion, the modelling of perturbations is key for the construction of accurate linearised relative motion models as well as relative orbit design; both of which play a paramount role in the constantly growing discipline of distributed space systems.

Research outlook and future work.

The very wide horizon in which this topic is framed leads for countless possible research areas.

The evaluation of a robust implementation of Kaula's theory is the first on the list. This would be followed by an analysis of the resonant and secular terms, such as done by Chao [17]. The development of mean-to-osculating transformations through this theory is also considered, which could

derive into the development of linear relative motion models based on it.

In a somewhat more general sense, the survey, analysis and implementation of perturbed relative motion models (STMs) is to be tackled. A performance analysis of these models against a High-Fidelity and unperturbed models would be insightful, surely.

Orbit safety might also be an interesting topic to follow up on. A review of the existent models for non-circular, perturbed reference orbits would be insightful, and would continue on the here developed models for simpler cases (*i.e.* circular perturbed and elliptic unperturbed).

Further down the road, other types of perturbations might be analyzed, through the averaging methods here presented. Third bodies or drag are the most relevant ones, although second-order NSG effects are also to be considered.

Finally, real world scenarios may be analyzed, and eventually, a self-contained tool for this purpose could be regarded. Hopefully, this sort of roadmap looks as compelling as it does to the author.

Absolute and relative orbital element sets.

A.1 Introduction.

The description of a spacecraft's state is done via a state vector. While it can include several variables with other purposes (*e.g.* filtering), its only information throughout this thesis is the position and velocity. There are two main ways to describe them:

   A. Through **cartesian coordinates**

   B. Through **orbital elements**

While the first option yields a very explicit and graphic-ready description, the second one usually has two advantages over it. Firstly, orbital elements are generally more intuitive about both the orbit and the position on it. Secondly, as orbital elements are generally slow-varying, they allow for a bigger integration timestep without losing accuracy. This is quite clear when studying keplerian motion, as most of the elements remain constant. Variational formulation and Hamilton-Jacobi theory (with the notion of changing variables as the full solution of a problem) relate to this fact.

Throughout this thesis, several sets of orbital elements have been used. The goal of this appendix is to clarify on the definition and differences between them. Absolute orbital elements (OEs) will be described first, followed by relative OEs (ROEs).

A.2 Absolute element sets.

A.2.1 Workflow for transformations between absolute element sets.

Consider two different sets of OEs, denoted by $\underline{OE}$ and $\widetilde{\underline{OE}}$. The transformation function $\boldsymbol{G}_{OE \to \widetilde{OE}}$ between them is defined by:

$$\widetilde{\underline{OE}} = \boldsymbol{G}_{OE \to \widetilde{OE}}(\underline{OE}) \tag{A.1}$$

A numerous amount of element sets have been historically defined. Nevertheless, some of them are much more commonly used than others. Although this analysis will be restricted to a short number of sets (say n), the number of transformations becomes arduously large as n increases ($n(n-1)$).

In order to reduce the number of transformation functions $\boldsymbol{G}$, the later defined Keplerian OEs (KOEs) will be used as a pivot, that is, building only transformations to and from KOEs. This will in turn reduce the number of required functions to $2n$. The Keplerian set also has a further advantage: as it is the classical element set, almost every other set is defined explicitly in terms of it, so that transformations to and from them can be easily derived. A simple, graphical explanation of this is shown in figure A.1.

$$\widetilde{OE} \rightarrow \boxed{\widetilde{OE} \Rightarrow KOE} \rightarrow KOE \rightarrow \boxed{KOE \Rightarrow \overset{\star}{OE}} \rightarrow \overset{\star}{OE}$$

Figure A.1: Workflow for transforming between two arbitary absolute element sets.

A.2.2   Element sets.

A.2.2.1   Keplerian orbital elements (KOE).

The Keplerian set of OEs (KOE) is one of the most widely used and classic options. An usual definition is the following:

$$
\begin{cases}
a & \equiv & \text{Semimajor axis} & [L] \\
e & \equiv & \text{Eccentricity} & [--] \\
i & \equiv & \text{Inclination} & [rad] \\
\Omega \text{ or } RAAN & \equiv & \text{Right ascension of the ascending node} & [rad] \\
\omega & \equiv & \text{Argument of periapsis} & [rad] \\
M & \equiv & \text{Mean anomaly} & [rad]
\end{cases}
\tag{A.2}
$$

The last element commonly varies across literature, being substituted by the true anomaly θ; or, when tackling the variation of orbital parameters, by the mean anomaly at $t = 0$ (M_0) or the perigee time T_0 [18]. Mean anomaly is used due to the simplicity of its unperturbed variational equation, as it has a constant rate (denoted by n). The geometrical meaning and definition of these elements is out from the scope of this thesis. Nonetheless, figure A.2 shows a simple geometrical drawing of the involved angles.
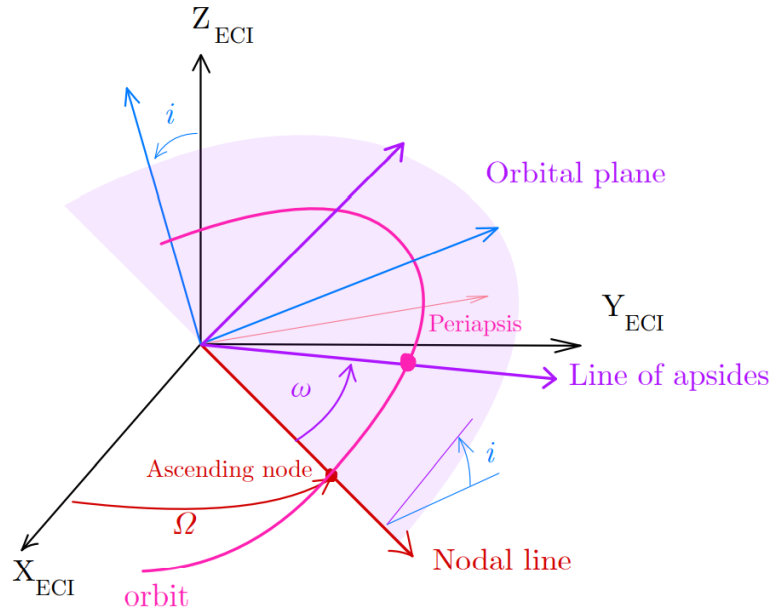
Figure A.2: Frame rotation from inertial to perifocal frame.

As it is seen in the figure before, the Keplerian elements become singular in two cases:

A. If the **inclination** is null, the orbital plane is coincident with the inertial reference (ECI x-y) plane. The ascending node is hence undefined in this case.

B. If the **eccentricity** is null, the periapsis is not defined, as it is the nearest point of the orbit around the central body. Thus, there is no angle defining its position, making the argument of periapsis singular.

These singularities are unfortunately quite common in orbit design. They correspond respectively with equatorial and circular orbits. In order to avoid this behaviour, many different elements sets have been defined. Wiesel [18] shows an intuitive approach in section 2.10, solving either problem with a graphic approach.

A.2.2.2   Eccentricity/inclination vectors orbital elements (EIOE).

This set, originally defined for geostationary orbits in absolute terms [19], is used mainly as a relative OE set. Though it is actually not used along this thesis, its definition is helpful for introducing the relative counterpart.

I.Eccentricity vector.

The notion of the eccentricity vector is quite basic, as it is, when in unperturbed motion, a constant

of the dynamic system. It is defined as the eccentricity-sized vector pointing towards the perigee. Nonetheless, for this purpose, the eccentricity vector is defined as [20]:

$$
\underline{e} = \left\{ \begin{array}{c} e_x \\ e_y \end{array} \right\} = e \left\{ \begin{array}{c} \cos \varpi \\ \sin \varpi \end{array} \right\} \tag{A.3}
$$

where the argument of perigee ω might be substituted with the sum $\omega + \Omega$ [as in 19]. A graphical representation can be seen later in the relative definition A.5(a). As it arises from (A.3), it substitutes the eccentricity and argument of perigee from the Keplerian OE set.

II. Inclination vector.

The inclination vector is perpendicular to the orbital plane, similarly to the angular momentum, but inclination-sized. It is defined by its components as [19]:

$$
\underline{i} = \left\{ \begin{array}{c} i_x \\ i_y \end{array} \right\} = i \left\{ \begin{array}{c} \cos \Omega \\ \sin \Omega \end{array} \right\}
$$

The graphical interpretation is not as straightforward as for the eccentricity vector. It is clear that these components substitute the out-of-plane related elements i and Ω.

III. Element set.

The EI orbital element set is then composed of:

$$
\left\{ \begin{array}{lll} a & \equiv \text{ Semimajor axis} & [L] \\ e_x = e \cos \omega & \equiv \text{ x-projection of } \underline{e} & [--] \\ e_y = e \sin \omega & \equiv \text{ y-projection of } \underline{e} & [--] \\ i_x = i \ \cos \Omega & \equiv \text{ x-component of } \underline{i} & [--] \\ i_y = i \ \sin \Omega & \equiv \text{ y-component of } \underline{i} & [--] \\ \lambda = \omega + M & \equiv \text{ Mean argument of latitude} & [rad] \end{array} \right. \tag{A.4}
$$

A.2.2.3 Quasi-nonsingular orbital elements (QNSOE).

The quasi-nonsingular (QNS) orbital element set tackles the singularity existing in circular orbits [21], [22] [23]. It is quite similar to the formerly defined EI set, as it uses again the components

of the eccentricity vector to substitute e and ω. The set is then defined as:

$$
\begin{cases}
a & \equiv & \text{Semimajor axis} & [L] \\
q_1 = e \cos\omega & \equiv & \text{x-projection of } \underline{e} & [--] \\
q_2 = e \sin\omega & \equiv & \text{y-projection of } \underline{e} & [--] \\
i & \equiv & \text{Inclination} & [rad] \\
\Omega & \equiv & \text{Right ascension of the ascending node} & [rad] \\
\lambda = \omega + M & \equiv & \text{Mean argument of latitude} & [rad]
\end{cases}
\tag{A.5}
$$

Though some authors use a different order, this is the one used in this thesis, so as to keep the time-varying element on the last place.

A.2.2.4   Equinoctial orbital elements (EOE).

The QNS set of elements only solved half of the singularity problem. To solve both, thus enabling the description of equatorial and polar orbits, the equinoctial set of elements is defined as:

$$
\begin{cases}
a & \equiv & \text{Semimajor axis} & [L] \\
P_1 = e \cos\varpi & \equiv & \textit{unclear physical meaning, similar to } e_x & [--] \\
P_2 = e \sin\varpi & \equiv & \textit{unclear physical meaning, similar to } e_y & [--] \\
Q_1 = \tan\frac{i}{2}\cos\Omega & \equiv & \textit{unclear physical meaning, similar to } i_x & [--] \\
Q_2 = \tan\frac{i}{2}\sin\Omega & \equiv & \textit{unclear physical meaning, similar to } i_y & [--] \\
L = \Omega + \omega + \theta & \equiv & \text{True longitude} & [rad]
\end{cases}
\tag{A.6}
$$

where $\varpi = \Omega + \omega$. Not only does the order does change depending on the author, but also the symbols to refer to them. An example of its use is [21].

A.2.2.5   Delaunay orbital elements (DOE).

Delaunay elements arise when formulating the two-body problem through analytical mechanics **??**. Conversely to the previous element sets, who are clearly non-canonical (*i.e.* they do not satisfy Hamilton's equations), Delaunay elements are built based on the analytical perspective of the problem. Starting from the canonical set of elements (see appendix **??**), Delaunay elements are reached after

performing a canonical transformation, leading to the following definition:

$$
\begin{cases}
L = \sqrt{\mu\,a} & \equiv & \textit{unclear physical meaning} & [L^{1/2}] \\
G = L\sqrt{1 - e^2} & \equiv & \text{Angular momentum} & [L^{1/2}] \\
H = G\cos i & \equiv & \text{Polar component of angular momentum} & [L^{1/2}] \\
l = M & \equiv & \text{Mean anomaly} & [rad] \\
g = \omega & \equiv & \text{Argument of perigee} & [rad] \\
h = \Omega & \equiv & \text{Right ascension of ascending node} & [rad]
\end{cases}
\tag{A.7}
$$

This set is mainly used in the context of perturbations, as it yields a very convenient expression for the perturbed Hamiltonian (see section **??**).

A.3   Relative sets.

Relative elements are at the deepest roots of spacecraft relative motion, offering several advantages over cartesian relative states. First and foremost, they are more intuitive, but they also lead to a reduction of linearisation errors when expanding the deputy's movement around the chief's orbit [24]. In general, relative elements are defined as:

$$
\delta\underline{OE} = \boldsymbol{f}\left(\underline{OE_C}, \underline{OE_D}\right)
\tag{A.8}
$$

which is usually simplified by just taking the arithmetic difference between them, namely

$$
\delta\underline{OE} = \underline{OE_D} - \underline{OE_C}
\tag{A.9}
$$

where the subscripts denote respectively the deputy and chief spacecraft. The question now is, how do transformations between ROEs work.

A.3.1   Workflow for transformations between ROEs.

As for the absolute elements, Keplerian elements will be used as a pivot point. That means that only the transformations from and to RKOEs must be implemented. There are then two types of transformations:

A) From any ROE set to RKOE

While authors provide with scenarios expressed in their own ROE set, the element choice for this thesis is the Keplerian set. That leads to the need of implementing a transformation from the former set to the latter. The considered inputs and outputs are:

- **Inputs**:

  - $\widetilde{\underline{ROE}} = \delta\widetilde{\underline{OE}}$: Any type of ROEs, whose absolute equivalents are known as a function of the KOEs ($\widetilde{\underline{OE}} = \boldsymbol{f}(\underline{KOE})$)

  - $\underline{KOE}_C$: Chief spacecraft/reference orbit KOEs

- **Output**:

  - $\underline{RKOE} = \delta\underline{KOE}$: Keplerian ROEs

Taking equation (A.9) and particularizing it for KOEs:

$$\delta\underline{KOE} = \underline{KOE}_D - \underline{KOE}_C \tag{A.10}$$

while the second term is known (input), the second one must be calculated through a certain process:

1st Calculate chief's OEs in the source phase space (*i.e.* $\widetilde{\underline{OE}}_C$)

$$\widetilde{\underline{OE}}_C = \boldsymbol{G}_{KOE \to \widetilde{OE}}(\underline{KOE}_C)$$

2nd Compute deputy's OEs by direct addition

$$\widetilde{\underline{OE}}_D = \widetilde{\underline{OE}}_C + \delta\widetilde{\underline{OE}}$$

3rd Compute deputy's KOEs by back-transformation

$$\underline{KOE}_D = \boldsymbol{G}_{\widetilde{OE} \to KOE}(\underline{OE}_D)$$

4th Subtract chief's KOEs from deputy's

$$\delta\underline{KOE} = \underline{KOE}_D - \underline{KOE}_C$$

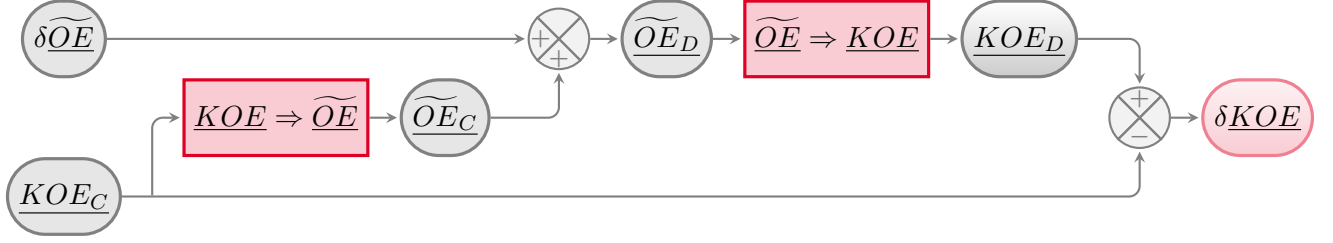See graphic A.3 for a more visual explanation.

Figure A.3: Workflow for transforming any relative set into KOE.

B) From RKOE to any ROE set

In this case, the assumed inputs and outputs are:

- **Inputs:**

    - $\underline{RKOE} = \delta\underline{KOE}$: Keplerian ROEs

    - $\underline{KOE_C}$: Chief KOEs

- **Output**:

    - $\widetilde{\underline{ROE}} = \delta\widetilde{\underline{OE}}$: Any type of ROEs, whose absolute equivalents are known as a function of the KOEs ($\widetilde{\underline{OE}} = \underline{f}\,(\underline{KOE})$)

For this transformation, the equation A.8 particularized for this case acquires the following shape:

$$\delta\widetilde{\underline{OE}} = \widetilde{\underline{OE_D}} - \widetilde{\underline{OE_C}} \tag{A.11}$$

Equation A.11 can be tackled in two main ways:

A. Using the pertinent transformations, compute the absolute elements for both spacecrafts $\widetilde{\underline{OE_D}}$, $\widetilde{\underline{OE_C}}$, and then calculate the arithmetic difference (in a A.3.1). See graphic A.4.

B. Expand the deputy absolute OEs (*i.e.* $\widetilde{\underline{OE_D}}$) around the chief via a Taylor series expansion with respect to the Keplerian set of elements, retaining terms up to first order, achieving a linearised expression for the transformation. Mathematically:

$$\widetilde{\underline{OE_D}} = \widetilde{\underline{OE}}(\underline{KOE_D}) = \widetilde{\underline{OE}}(\underline{KOE_C} + \delta\underline{KOE})) = \widetilde{\underline{OE_C}} + \frac{\partial\widetilde{\underline{OE}}}{\partial\underline{KOE}}\delta\underline{KOE} + \mathcal{O}\left(\delta\underline{KOE}^2\right)$$
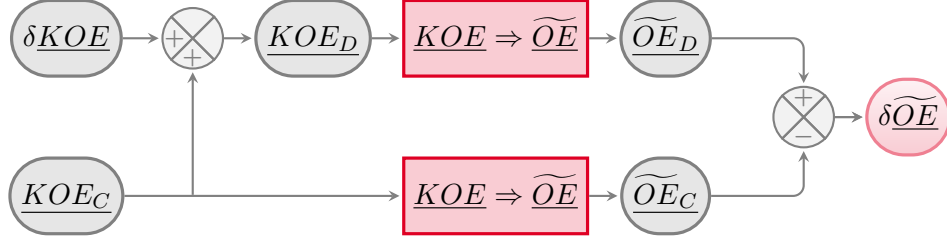
Figure A.4: Workflow for transforming RKOE into any other set.

hence,

$$\delta\widetilde{OE} \approx \widetilde{\underline{OE_C}} + \frac{\partial\widetilde{\underline{OE}}}{\partial\underline{KOE}}\delta\underline{KOE} - \widetilde{\underline{OE_C}} = \frac{\partial\widetilde{\underline{OE}}}{\partial\underline{KOE}}\delta\underline{KOE} \tag{A.12}$$

where the Jacobian matrix is generally simple, as it usually only implies polynomic or trigonometric functions. Equation (A.12) is then a first order approximation of (A.11). Its validity is then reduced to a close proximity between both spacecrafts, which should be assessed.

A.3.2 Element sets.

Besides the ones derived directly from its absolute counterparts, a couple of additional ROE sets will be herewith defined and explained. This is due to one of two reasons. The first one is that some ROE sets are only defined in relative terms, lacking any absolute equivalent. The second one is that it might be interesting to dive in the meaning of the relative sets, deriving interesting relations that would otherwise be overlooked.

A.3.2.1 Relative eccentricity/inclination vectors orbital elements (REIOE).

This ROE set is the counterpart of the EI set (see A.2.2.2). It is nonetheless interesting to see the meaning and shape of it, as it is quite widely used in literature [20, 22, 23]. Firstly, the elements themselves are defined, to later analyze the meaning behind them:

$$\begin{cases} \delta a & \equiv \text{ Relative semimajor axis} & [L] \\ \delta e_x & \equiv \text{ x-component of } \delta\underline{e} & [--] \\ \delta e_y & \equiv \text{ y-component of } \delta\underline{e} & [--] \\ \delta i_x & \equiv \text{ x-component of } \delta\underline{i} & [--] \\ \delta i_y & \equiv \text{ y-component of } \delta\underline{i} & [--] \\ \delta\lambda & \equiv \text{ Relative mean argument of latitude} & [rad] \end{cases} \tag{A.13}$$

(a) Relative eccentricity vector.

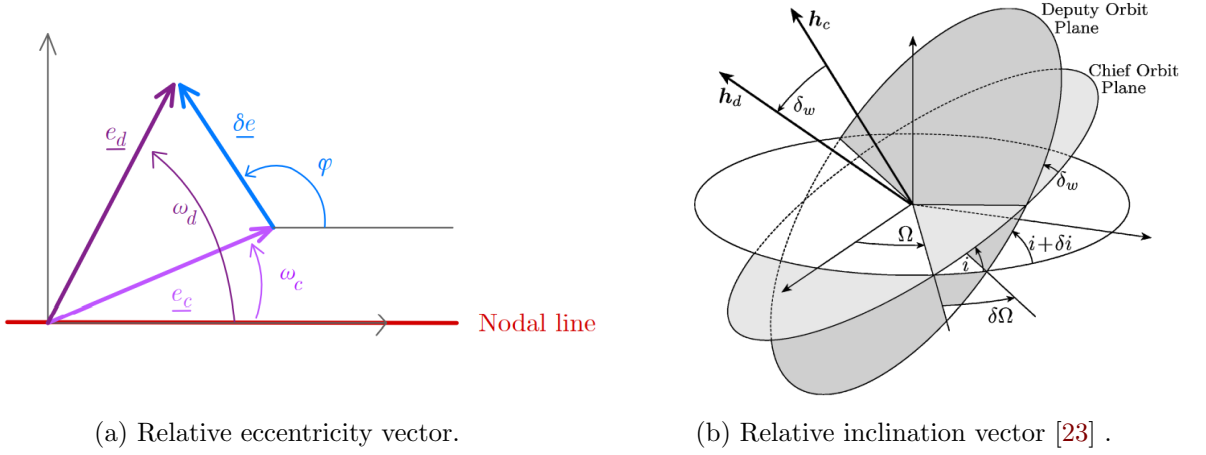(b) Relative inclination vector [23] .

Figure A.5: Relative ccentricity & inclination vectors.

Concept & meaning

The relative eccentricity vector components substitute the relative eccentricity and the relative argument of perigee. It is based on the eccentricity vector definition (A.3), and a graphical representation can be seen in figure A.5(a). Mathematically:

$$\delta\underline{e} = \left\{ \begin{array}{c} \delta e_x \\ \\ \delta e_y \end{array} \right\} = \delta e \left\{ \begin{array}{c} \cos\varphi \\ \\ \sin\varphi \end{array} \right\}$$

where φ is referred to as the AOP of the relative orbit. This vector rules the in-plane relative motion (hand in hand with δa and $\delta\lambda$). There are two ways of tackling the transformation from RKOE to this set (see A.3.1). Besides the exact nonlinear form, a linear version can be derived. Assuming that the difference in the eccentricity vector is due to that of the eccentricity and argument of perigee (δe, $\delta\omega$), it follows that:

$$\delta\underline{e} \approx \left[\begin{array}{cc} \cos\omega & -e\sin\omega \\ \\ \sin\omega & e\cos\omega \end{array} \right] \left\{ \begin{array}{c} \delta e \\ \\ \delta\omega \end{array} \right\} \tag{A.14}$$

where terms of second order and higher have been neglected. The relative inclination vector is defined in an alternative way [20] (comparing with the absolute counterpart). Mathematically:

$$\delta \underline{i} = \sin \delta i \left\{ \begin{array}{c} \cos \theta \\ \\ \sin \theta \end{array} \right\}$$

where θ is the analogue angle to φ in the eccentricity vector, being commonly referred to as the RAAN of the relative orbit. Once again, the linearised transformation from RKOE to this set may be analysed, considering the differences δi and $\delta \Omega$. Applying the law of sines and the law of cosines for spherical trigonometry and assuming small values of δi and $\delta \Omega$, it follows that:

$$\delta \underline{i} = \left\{ \begin{array}{c} \delta i \\ \\ \sin i \delta \Omega \end{array} \right\} \approx \left[\begin{array}{cc} 1 & 0 \\ \\ 0 & \sin i \end{array} \right] \left\{ \begin{array}{c} \delta i \\ \\ \delta \Omega \end{array} \right\} \tag{A.15}$$

where i is the inclination of the chief's orbit. Combining the results of (A.14) and (A.15) with the definitions of the remaining elements, an expression analogue to (A.12) is reached:

$$\left\{ \begin{array}{c} \delta a \\ \delta e_x \\ \delta e_y \\ \delta i_x \\ \delta i_y \\ \delta \lambda \end{array} \right\} \approx \left[\begin{array}{cccccc} 1 & 0 & 0 & 0 & 0 & 0 \\ 0 & \cos \omega & 0 & 0 & -e \sin \omega & 0 \\ 0 & \sin \omega & 0 & 0 & e \cos \omega & 0 \\ 0 & 0 & 1 & 0 & 0 & 0 \\ 0 & 0 & 0 & \sin i & 0 & 0 \\ 0 & 0 & 0 & 0 & 1 & 1 \end{array} \right] \left\{ \begin{array}{c} \delta a \\ \delta e \\ \delta i \\ \delta \Omega \\ \delta \omega \\ \delta M \end{array} \right\} \tag{A.16}$$

A graphical representation of this concept can be seen in figure A.5(b).

However, this definition is changed in some references. In particular, the mean argument of latitude λ is sometimes substituted by the modified relative mean longitude, which is defined as:

$$\delta l_0 \equiv \delta \lambda + \delta \Omega \cos i$$

The advantage of this formulation is that the in-plane motion becomes decoupled. This will also be done in the following set of relative elements.

A.3.2.2   C set of relative orbital elements (CROE).

Defined by Peters & Noomen in [25], this set is also closely related with the orbit safety notion. It arises from the analysis of the Gauss Variational Equations (GVEs) applied to the relative dynamics between a deputy and a chief spacecraft, when the former performs a cotangential transfer. The elements themselves are defined as:

$$
\begin{cases}
C_1 = \delta p = \eta^2 \delta a - 2\,a\,e\delta e & \equiv & \text{Relative parameter of the orbit} & [L] \\[2mm]
C_2 = e\delta p - p\delta e & \equiv & \textit{unclear physical meaning} & [L] \\[2mm]
C_3 = -e\,p\,(\delta\omega + \cos i\delta\Omega) & \equiv & \textit{unclear physical meaning} & [L] \\[2mm]
C_4 = a\left(\delta\omega + \cos i\delta\Omega + \eta^{-1}\delta M\right) & \equiv & \text{Modified relative mean longitude} & [L] \\[2mm]
C_5 = -p\,(\cos\omega\delta i + \sin i \sin\omega\delta\Omega) & \equiv & \textit{unclear physical meaning} & [L] \\[2mm]
C_6 = p\,(\sin\omega\delta i - \sin i \cos\omega\delta\Omega) & \equiv & \textit{unclear physical meaning} & [L]
\end{cases}
\tag{A.17}
$$

For a proper geometrical and conceptual description of the elements, please see [25]. As an introduction, the first four elements essentially determine the in-plane relative motion. C_1, C_2 & C_3 arise from a very intelligent interpretation of the GVEs, with C_4 completing the element set. On the other hand, elements C_5 and C_6 describe the out-of-plane motion.

Bibliography

[1]   S. Marsland. *Machine Learning: An Algorithmic Perspective*. 2nd ed. Boca Raton, USA: Chapman & Hall/CRC, 2015 (cit. on pp. 1, 3).

[2]   D. Barrett et al. "Measuring abstract reasoning in neural networks". In: *Proceedings of the 35th International Conference on Machine Learning*. Ed. by J. Dy and A. Krause. Vol. 80. Proceedings of Machine Learning Research. PMLR, Oct. 2018, pp. 511–520. URL: https://proceedings.mlr.press/v80/barrett18a.html (cit. on p. 3).

[3]   B. M. Lake and M. Baroni. "Still not systematic after all these years: On the compositional skills of sequence-to-sequence recurrent networks". In: *CoRR* abs/1711.00350 (2017). arXiv: 1711.00350. URL: http://arxiv.org/abs/1711.00350 (cit. on p. 3).

[4]   D. Saxton et al. "Analysing Mathematical Reasoning Abilities of Neural Models". In: *CoRR* abs/1904.01557 (2019). arXiv: 1904.01557. URL: http://arxiv.org/abs/1904.01557 (cit. on p. 3).

[5]   T. Ebert, J. Belz, and O. Nelles. "Interpolation and extrapolation: Comparison of definitions and survey of algorithms for convex and concave hulls". In: *2014 IEEE Symposium on Computational Intelligence and Data Mining (CIDM)*. IEEE. 2014, pp. 310–314 (cit. on p. 3).

[6]   W.-Y. Loh, C.-W. Chen, and W. Zheng. "Extrapolation errors in linear model trees". In: *ACM Transactions on Knowledge Discovery from Data (TKDD)* 1.2 (2007), 6–es (cit. on p. 3).

[7]   P. Klesk. "Construction of a Neurofuzzy Network Capable of Extrapolating (and Interpolating) With Respect to the Convex Hull of a Set of Input Samples in R". In: *IEEE Transactions on Fuzzy Systems* 16.5 (2008), pp. 1161–1179. DOI: 10.1109/TFUZZ.2008.924337 (cit. on p. 3).

[8]   R. Balestriero, J. Pesenti, and Y. LeCun. "Learning in high dimension always amounts to extrapolation". In: *arXiv preprint arXiv:2110.09485* (2021) (cit. on pp. 3, 4).

[9]   F. P. Preparata and M. I. Shamos. "Convex Hulls: Basic Algorithms". In: *Computational Geometry: An Introduction*. New York, NY: Springer New York, 1985, pp. 95–149. ISBN: 978-1-4612-1098-6. DOI: 10.1007/978-1-4612-1098-6_3. URL: https://doi.org/10.1007/978-1-4612-1098-6_3 (cit. on p. 3).

[10] I. Bárány and Z. Füredi. "On the shape of the convex hull of random points". In: *Probability theory and related fields* 77 (1988), pp. 231–240 (cit. on p. 4).

[11]   L. Bonnasse-Gahot. "Interpolation, extrapolation, and local generalization in common neural networks". In: *arXiv preprint arXiv:2207.08648* (2022) (cit. on p. 4).

[12]   O. Montenbruck and E. Gill. *Satellite Orbits: Models, Methods and Applications.* 1st ed. Wessling, Germany: Springer, 2001 (cit. on p. 5).

[13]   K. Yamanaka and F. Ankersen. "New State Transition Matrix for Relative Motion on an Arbitrary Elliptical Orbit". In: *Journal of Guidance, Control & Dynamics* 25.1 (2002), pp. 60–66. DOI: 10.2514/2.4875 (cit. on p. 6).

[14]   D.-W. Gim and K. Alfriend. "State Transition Matrix of Relative Motion for the Perturbed Noncircular Reference Orbit". In: *Journal of Guidance Control and Dynamics* 26 (Nov. 2003), pp. 956–971. DOI: 10.2514/2.6924 (cit. on p. 6).

[15]   S.-S. Exchange. *Practical Uses of an STM.* 2019. URL: https://space.stackexchange.com/questions/32916 (cit. on p. 7).

[16]   ESA. *Precise Orbit Determination.* 2011. URL: https://gssc.esa.int/navipedia/index.php/Precise_Orbit_Determination (cit. on p. 7).

[17]   C. Chao and F. Hoots. *Applied Orbit Perturbation and Maintenance.* Aerospace Press, 2018. ISBN: 9781523123346 (cit. on p. 11).

[18]   W. E. Wiesel. *Modern Astrodynamics.* 2nd ed. Beavercreek, Ohio: Aphelion Press, 2010 (cit. on pp. 14, 15).

[19]   M. Eckstein, C. Rajasingh, and P. Blumer. "Colocation Strategy and Collision Avoidance for the Geostationary Satellites at 19 Degrees West". In: *CNES International Symposium on Space Dynamics.* Vol. 25. Oberpfaffenhofen, Germany: DLR GSOC, Nov. 1989, pp. 60–66 (cit. on pp. 15, 16).

[20]   S. D'Amico and O. Montenbruck. "Proximity Operations of Formation-Flying Spacecraft Using an Eccentricity/Inclination Vector Separation". In: *Journal of Guidance, Control & Dynamics* 29.3 (2006), pp. 554–563. DOI: 10.2514/1.15114 (cit. on pp. 16, 21, 23).

[21]   D.-W. Gim and K. T. Alfriend. "Satellite Relative Motion Using Differential Equinoctial Elements". In: *Celestial Mechanics and Dynamical Astronomy* 92.4 (2005), pp. 295–336. DOI: 10.1007/s10569-004-1799-0 (cit. on pp. 16, 17).

[22] S. D'Amico. *Relative Orbital Elements as Integration Constants of Hill's Equations*. TN 05-08. Oberpfaffenhofen, Germany: Deutsches Zentrum für Luft- und Raumfahrt (DLR), 2005 (cit. on pp. 16, 21).

[23] H. Schaub. "Relative Orbit Geometry Through Classical Orbit Element Differences". In: *Journal of Guidance, Control & Dynamics* 27.5 (2004), pp. 839–848. DOI: `10.2514/1.12595` (cit. on pp. 16, 21, 22).

[24] G. Gaias, C. Colombo, and M. Lara. "Accurate Osculating/Mean Orbital Elements Conversions for Spaceborne Formation Flying". In: (Feb. 2018). `https://www.researchgate.net/publication/340378956_Accurate_OsculatingMean_Orbital_Elements_Conversions_for_Spaceborne_Formation_Flying` (cit. on p. 18).

[25] T. Vincent Peters and R. Noomen. "Linear Cotangential Transfers and Safe Orbits for Elliptic Orbit Rendezvous". In: *Journal of Guidance, Control & Dynamics* 44.4 (2021), pp. 732–748. DOI: `10.2514/1.G005152` (cit. on p. 24).

[26] B. D. Tapley, B. E. Schutz, and G. H. Born. *Statistical Orbit Determination*. 1st ed. Amsterdam, Netherlands: Elsevier, 2004.

[27] K. T. Alfriend and Srinivas. *Spacecraft Formation Flying*. 1st ed. Oxford, United Kingdom: Elsevier, 2010.

[28] R. H. Battin. *An Introduction to the Mathematics and Methods of Astrodynamics, Revised Edition*. 1st ed. Reston, Virginia: American Institute of Aeronautics and Astronautics, 1999.

[29] D. Brouwer and G. M-Clemence. *Methods of Celestial Mechanics*. Brackley Square House, London: Academic Press, 1961.

[30] H. Schaub and J. L. Junkins. *Analytical Mechanics of Space Systems*. Reston, VA: AIAA Education Series, Oct. 2003. DOI: `10.2514/4.861550`.

[31] W. Fehse. *Automated Rendezvous and Docking of Spacecraft*. Cambridge Aerospace Series. Cambridge: Cambridge University Press, 2003. DOI: `10.1017/CBO9780511543388`.

[32] P. K. S. Dennis D. McCarthy. *Time: From Earth Rotation to Atomic Physics*. Wiley-VCH, 2009. ISBN: 3527407804; 9783527407804.

[33] K. Wakker. *Fundamentals of Astrodynamics*. Jan. 2015. ISBN: 978-94-6186-419-2.

[34] A. H. Nayfeh. *Perturbation Methods*. Weinheim, Germany: Wiley-VCH, 2004.

[35] W. M. Kaula. *Theory of Satellite Geodesy*. Mineola, New York: Dover Publications, 2013.

[36]   F. Tisserand. *Traité de Mécanique Céleste*. Vol. 1. Paris, 1889.

[37]   J. Sullivan, S. Grimberg, and S. D'Amico. "Comprehensive Survey and Assessment of Spacecraft Relative Motion Dynamics Models". In: *Journal of Guidance, Control & Dynamics* 40.8 (2017), pp. 1837–1859. DOI: 10.2514/1.G002309.

[38]   H. Schaub and K. T. Alfriedn. "Hybrid Cartesian and Orbit Element Feedback Law for Formation Flying Spacecraft". In: *Journal of Guidance, Control & Dynamics* 25.2 (2002), pp. 387–393. DOI: 10.2514/2.4893.

[39]   N. Capitaine. "The Celestial Pole Coordinates". In: *Celestial Mechanics and Dynamical Astronomy* 48 (1990), pp. 127–143.

[40]   D. D. McCarthy. *IERS Conventions (1992)*. 21. Paris, France: Central Bureau of IERS - Observatoire de Paris, 1996.

[41]   J. Williams. *LVLH Transformations*. https://degenerateconic.com/uploads/2015/03/lvlh.pdf. 2014.

[42]   H. Fiedler. *Analysis of TerraSAR-L Cartwheel Constellations*. https://elib.dlr.de/22345/. Oberpfaffenhofen, Germany: Deutsches Zentrum für Luft- und Raumfahrt (DLR), Nov. 2003.

[43]   G. W. Hill. "Researches in the Lunar Theory". In: *American Journal of Mathematics* 1.2 (1878), pp. 129–147. DOI: 10.2307/2369304.

[44]   W. H. Clohessy and R. S. Wiltshire. "Terminal Guidance System for Satellite Rendezvous". In: *Journal of the Aerospace Sciences* 27.9 (1960), pp. 653–658. DOI: 10.2514/8.8704.

[45]   R. Broucke. "On the Matrizant of the Two-Body Problem". In: *Astronomy and Astrophysics* 6 (June 1970), p. 173.

[46]   J. Tschauner and P. Hempel. "Optimale Beschleunigungsprogramme fÃ¼r das Rendezvous-Manöver". In: *Astronautica Acta* 10 (1964), pp. 296–307.

[47]   T. Carter. "State Transition Matrices for Terminal Rendezvous Studies: Brief Survey and New Example". In: *Journal of Guidance Control and Dynamics* 21 (Jan. 1998), pp. 148–155. DOI: 10.2514/2.4211.

[48]   O. Montenbruck, M. Kirschner, and S. D'Amico. "E/I-vector separation for safe switching of the GRACE formation". In: *Aerospace Science and Technology* 10 (2006), pp. 628–635. DOI: 10.1016/j.ast.2006.04.001.

[49] G. Gaias, J.-S. Ardaens, and C. Colombo. "Precise line-of-sight modelling for angles-only relative navigation". In: *Advances in Space Research* 67.11 (2021). Satellite Constellations and Formation Flying, pp. 3515–3526. DOI: `10.1016/j.asr.2020.05.048`.

[50] G. Gaias, C. Colombo, and M. Lara. "Analytical Framework for Precise Relative Motion in Low Earth Orbits". In: *Journal of Guidance, Control, and Dynamics* 43.5 (2020), pp. 915–927. DOI: `10.2514/1.G004716`.

[51] D. Brouwer. "Solution of the problem of artificial satellite theory without drag". In: *Astronomical Journal* 64.5 (Nov. 1959), p. 378. DOI: `10.1086/107958`.

[52] R. H. Lyddane. "Small eccentricities or inclinations in the Brouwer theory of the artificial satellite". In: *Astronomical Journal* 68 (Oct. 1963), p. 555. DOI: `10.1086/109179`.

[53] A. Deprit. "Canonical transformations depending on a small parameter". In: *Celestial Mechanics* 1.1 (Mar. 1969), pp. 12–30. DOI: `10.1007/BF01230629`.

[54] A. Deprit. "Delaunay Normalisations". In: *Celestial Mechanics* 26.1 (Jan. 1982), pp. 9–21. DOI: `10.1007/BF01233178`.

[55] G. Hori. "Theory of General Perturbation with Unspecified Canonical Variable". In: *Publications of the Astronomical Society of Japan* 18 (Jan. 1966), pp. 287–296.

[56] Y. Chihabi and S. Ulrich. "Spacecraft Formation Guidance Law using a State Transition Matrix With Gravitational, Drag and Third-Body Perturbations". In: Jan. 2020. DOI: `10.2514/6.2020-1460`.

[57] G. Gaias, J. Ardaens, and O. Montenbruck. "Model of J2 Perturbed Satellite Relative Motion with Time-Varying Differential Drag". In: *Celestial Mechanics and Dynamical Astronomy* (2015).

[58] A. Koenig, T. Guffanti, and S. D'Amico. "New State Transition Matrices for Relative Motion of Spacecraft Formations in Perturbed Orbits". In: Sept. 2016. DOI: `10.2514/6.2016-5635`.

[59] A. Biria and R. Russell. "A Satellite Relative Motion Model Including J2 and J3 via Vinti's Intermediary". In: Feb. 2016.

[60] K. Alfriend and H. Yan. "An Orbital Elements Based Approach to the Nonlinear Formation Flying Problem". In: Toulouse, France, Feb. 2016.

[61] Mathworks. *Convert complex diagonal form into real diagonal form.* 2022. URL: `https://www.mathworks.com/help/matlab/ref/cdf2rdf.html`.

[62] M. R. Delgado. *Lecture notes: Basics of Orbital Mechanics I*. Apr. 2008.

[63] F. G. Nievinski. *subtightplot*. https://www.mathworks.com/matlabcentral/fileexchange/39664-subtightplot. 2013.

[64] J. C. Lansey. *linspecer*. https://www.mathworks.com/matlabcentral/fileexchange/42673-beautiful-and-distinguishable-line-colors-colormap. 2015.

[65] Jan. *WindowAPI*. https://www.mathworks.com/matlabcentral/fileexchange/31437-windowapi. 2013.

[66] T. Davis. *Arrow3*. https://www.mathworks.com/matlabcentral/fileexchange/14056-arrow3. 2022.

[67] E. Duenisch. *latexTable*. https://www.mathworks.com/matlabcentral/fileexchange/44274-latextable. 2016.